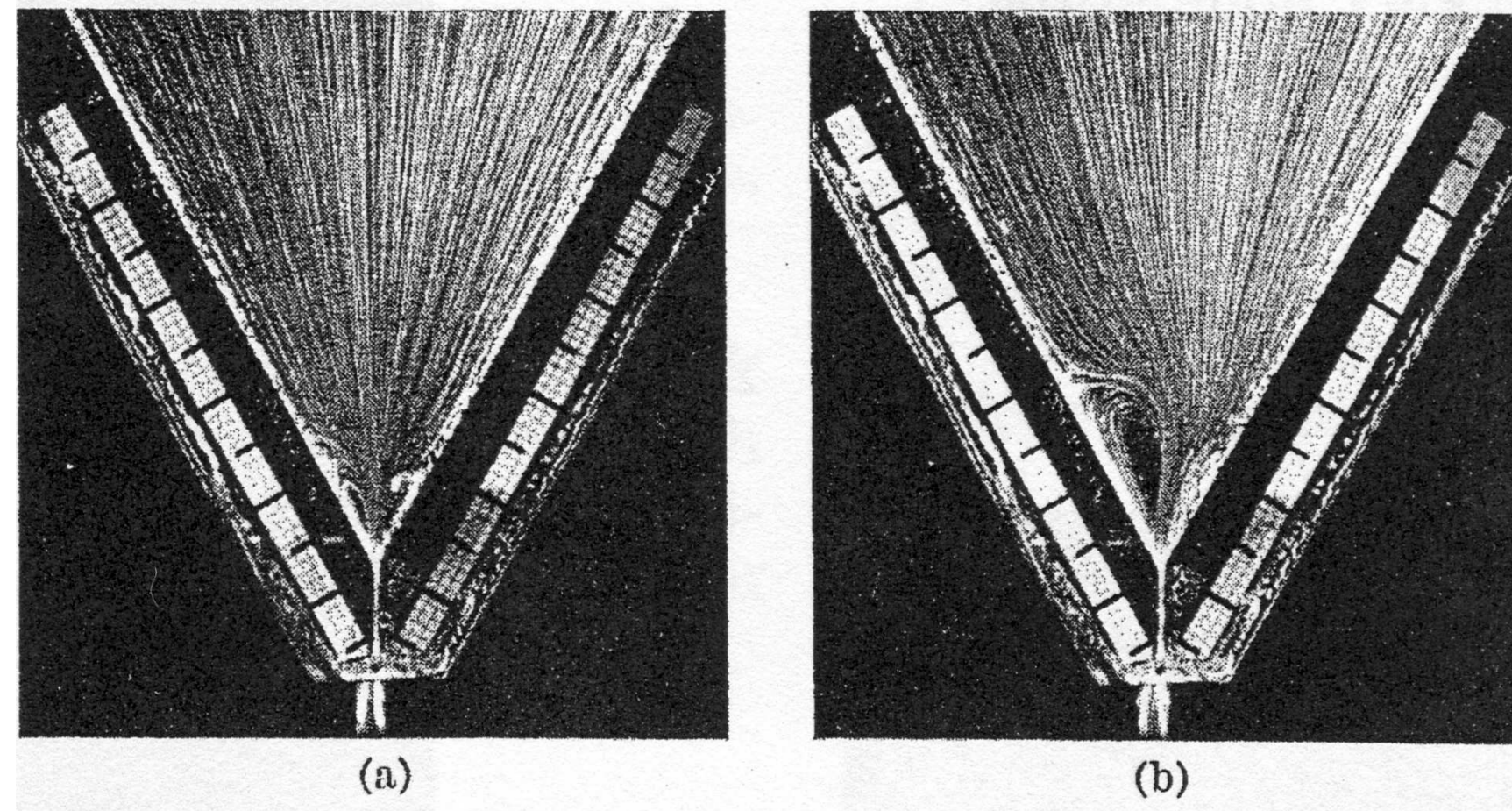


## Jeffery-Hamel Flow

The planar, steady flow of an incompressible viscous liquid in a wedge with a line sink is given by a purely radial flow: the Jeffery-Hamel solution of the Navier-Stokes equations.



H. Giesekus 1968, see [2]

For viscoelastic wedge flows little is known. A notable exception is the exact, radial solution found by Hull for the creeping sink flow of an upper convected Maxwell (UCM) fluid in a 180° wedge. Experimental work by Giesekus indicates that radial solutions are still important for viscoelastic liquids (Fig. a), but that viscoelasticity introduces strong nonlinear effects leading to flow recirculation and the occurrence of vortices (Fig. b), even for small Reynolds numbers.

**Problem:** Can we characterize the flow behavior of basic viscoelastic fluids near the wedge apex?

## The Governing Equations: UCM-Fluid

We consider the planar, steady, incompressible sink flow of a UCM fluid in a wedge. In dimensionless form, the governing equations are the momentum equation

$$\text{Re } \mathbf{v} \cdot \nabla \mathbf{v} = -\nabla p + \nabla \cdot \mathbf{T}, \quad (1)$$

the incompressibility condition

$$\nabla \cdot \mathbf{v} = 0 \quad (2)$$

and the constitutive relation

$$\mathbf{T} + \text{We } \overset{\nabla}{\mathbf{T}} = 2\mathbf{D}. \quad (3)$$

Here the rate-of-strain tensor is given by

$$\mathbf{D} = \frac{1}{2} (\nabla \mathbf{v} + (\nabla \mathbf{v})^T). \quad (4)$$

In these equations,  $\mathbf{T} = (T_{ij})$  is the extra stress tensor,  $\mathbf{v} = (v_r, v_\theta)^T$  is the velocity field (in cylindrical coordinates),  $p$  is the pressure, We is the Weissenberg number, and Re is the Reynolds number. The upper convected stress derivative is defined by

$$\overset{\nabla}{\mathbf{T}} = (\mathbf{v} \cdot \nabla) \mathbf{T} - (\nabla \mathbf{v}) \mathbf{T} - \mathbf{T} (\nabla \mathbf{v})^T. \quad (5)$$

**Problem:** Solve these equations in the two-dimensional sector  $0 < r < \infty$ ,  $0 \leq \theta \leq \pi/\alpha$  with  $\theta = 0$  and  $\pi/\alpha$  ( $\alpha \geq \frac{1}{2}$ ) representing solid walls of the wedge under the assumption of constant flux  $Q$ , where

$$Q = \int_0^{\pi/\alpha} v_r r d\theta = \psi \left( r, \frac{\pi}{\alpha} \right) - \psi(r, 0) \quad (6)$$

and  $\psi(r, \theta)$  is the two-dimensional (normalized) stream function ( $\psi = 0$  along the wall  $\theta = 0$ ).

**Note:** Scaling shows that it is sufficient to consider the case We = 1 (unless asymptotic regimes in terms of very large or very small We are discussed).

## Example: The (Global) Hull Solution

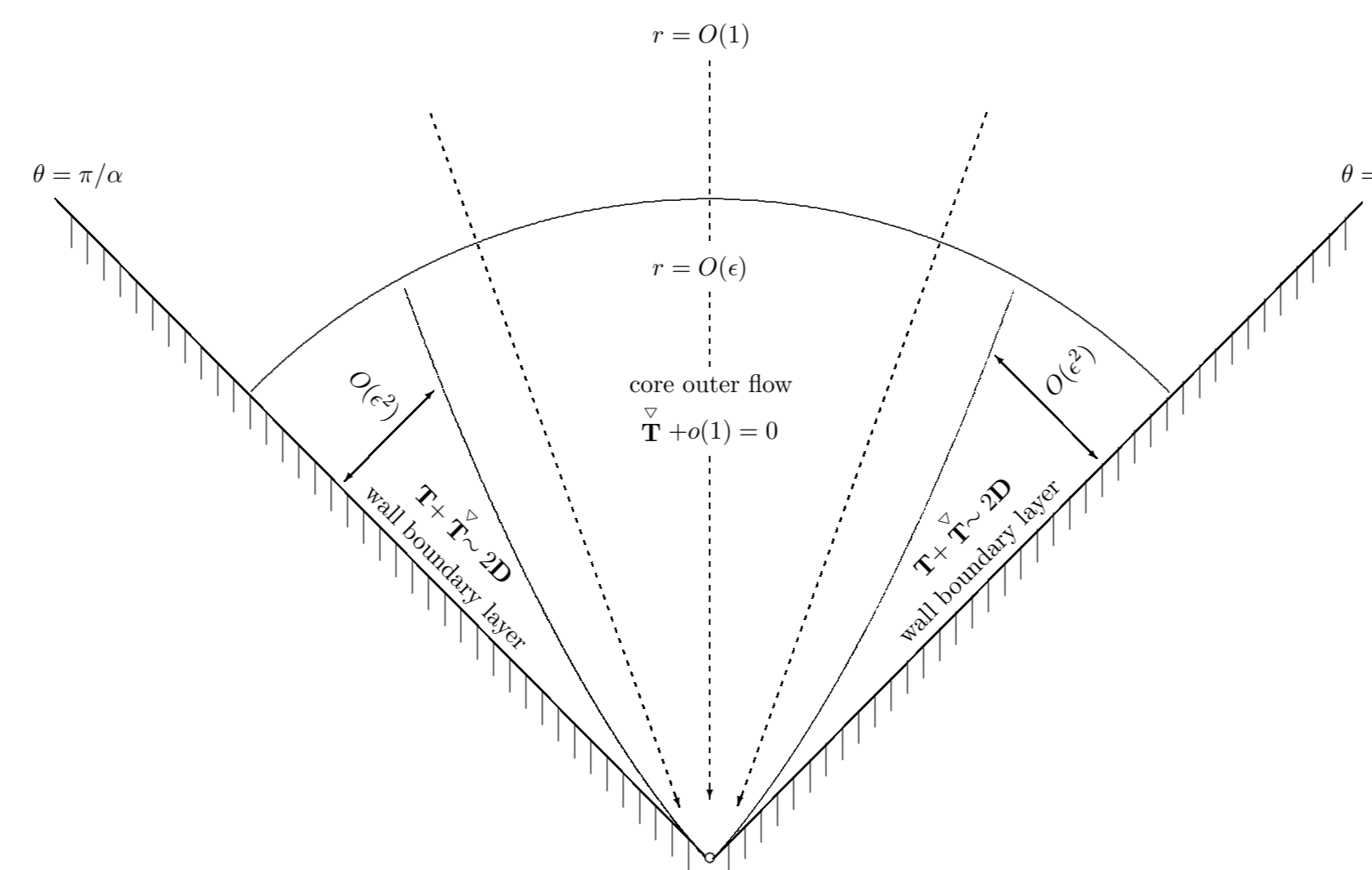
For the “wedge” with angle 180° ( $\alpha = 1$ ) and Re = 0, Hull [5] found the solution

$$\psi = \frac{Q}{2\pi} (2\theta - \sin(2\theta)). \quad (7)$$

This is the only known explicit solution, valid throughout the wedge.

## Asymptotics Near The Wedge Apex

Our asymptotic analysis separates the flow close to the wedge apex into a core flow region and a boundary layer region near the walls where stresses and velocities adjust to the core behavior.



## The Core Flow Outer Solution

The local balance in the constitutive equations is assumed to be  $\overset{\nabla}{\mathbf{T}} = o(1)$  as  $r \rightarrow 0$ , anticipating solutions in which the upper convected stress derivative dominates with the relaxation and rate-of-strain terms in (3) negligible. This behavior arises as a consequence of the sufficiently large stresses and velocity gradients expected near the apex.

Following Hinch [4] and Renardy [6], we find particular solutions to  $\overset{\nabla}{\mathbf{T}} = \mathbf{0}$  by setting

$$\mathbf{T} = (\lambda(\psi) + \text{Re}) \mathbf{v} \mathbf{v}^T \quad (8)$$

for an arbitrary function  $\lambda(\psi)$  of the stream function  $\psi$ . Further analysis reveals that

$$\psi = g(\theta) \quad (9)$$

solves then the momentum equation and incompressibility condition, where  $g$  is an arbitrary function of its argument, determining  $\lambda$  up to an arbitrary positive constant  $C_1$ . Because the flow is viscometric near the walls, we obtain

$$g(\theta) \sim C_0 \theta^3, \quad (10)$$

for some constant  $C_0$ , as the wall  $\theta = 0$  is approached. We thus have the wall behavior for the core solution in Cartesian form as

$$\psi \sim C_0 \frac{y^3}{x^3}, \quad p \sim p_0 x^{-2}, \quad T_{11} \sim C_1 x^{-2}, \quad T_{12} \sim C_1 \frac{y}{x^3}, \quad T_{22} \sim C_1 \frac{y^2}{x^4} \quad \text{for } y \rightarrow 0 \quad (11)$$

with some constants  $C_0$ ,  $C_1$  and  $p_0$ .

## Wall Boundary Layer Structure

Using an artificial small parameter  $\epsilon$ , we deduce the consistent set of scales

$$x = \epsilon \bar{X}, \quad y = \epsilon^2 \bar{Y}, \quad \psi = \epsilon^3 \bar{\Psi}, \quad p = \epsilon^{-2} \bar{p}, \quad T_{11} = \epsilon^{-2} \bar{T}_{11}, \quad T_{12} = \epsilon^{-1} \bar{T}_{12}, \quad T_{22} = \bar{T}_{22}. \quad (12)$$

In  $\bar{X} = O(1)$ ,  $\bar{Y} = O(1)$  we obtain, at leading order, Renardy's boundary layer equations [7]

$$0 = -\frac{d\bar{p}}{d\bar{X}} + \frac{\partial \bar{T}_{11}}{\partial \bar{X}} + \frac{\partial \bar{T}_{12}}{\partial \bar{Y}}, \quad (13)$$

$$\bar{T}_{11} + \left( \frac{\partial \bar{\Psi}}{\partial \bar{Y}} \frac{\partial \bar{T}_{11}}{\partial \bar{X}} - \frac{\partial \bar{\Psi}}{\partial \bar{X}} \frac{\partial \bar{T}_{11}}{\partial \bar{Y}} - 2 \frac{\partial^2 \bar{\Psi}}{\partial \bar{Y}^2} \bar{T}_{12} - 2 \frac{\partial^2 \bar{\Psi}}{\partial \bar{X} \partial \bar{Y}} \bar{T}_{11} \right) = 0, \quad (14)$$

$$\bar{T}_{22} + \left( \frac{\partial \bar{\Psi}}{\partial \bar{Y}} \frac{\partial \bar{T}_{22}}{\partial \bar{X}} - \frac{\partial \bar{\Psi}}{\partial \bar{X}} \frac{\partial \bar{T}_{22}}{\partial \bar{Y}} + 2 \frac{\partial^2 \bar{\Psi}}{\partial \bar{X}^2} + 2 \frac{\partial^2 \bar{\Psi}}{\partial \bar{X} \partial \bar{Y}} \bar{T}_{22} \right) = -2 \frac{\partial^2 \bar{\Psi}}{\partial \bar{X} \partial \bar{Y}}, \quad (15)$$

$$\bar{T}_{12} + \left( \frac{\partial \bar{\Psi}}{\partial \bar{Y}} \frac{\partial \bar{T}_{12}}{\partial \bar{X}} - \frac{\partial \bar{\Psi}}{\partial \bar{X}} \frac{\partial \bar{T}_{12}}{\partial \bar{Y}} + \frac{\partial^2 \bar{\Psi}}{\partial \bar{X}^2} \bar{T}_{11} - \frac{\partial^2 \bar{\Psi}}{\partial \bar{Y}^2} \bar{T}_{22} \right) = \frac{\partial^2 \bar{\Psi}}{\partial \bar{Y}^2}, \quad (16)$$

together with the wall conditions  $\bar{\Psi} = \frac{\partial \bar{\Psi}}{\partial \bar{Y}} = 0$  on  $\bar{Y} = 0$ , and the core flow matching conditions

$$\text{as } \bar{Y} \rightarrow \infty: \quad \bar{\Psi} \sim C_0 \frac{\bar{Y}^3}{\bar{X}^3}, \quad \bar{p} \sim p_0 \bar{X}^{-2}, \quad \bar{T}_{11} \sim C_1 \bar{X}^{-2}, \quad \bar{T}_{12} \sim C_1 \frac{\bar{Y}}{\bar{X}^3}, \quad \bar{T}_{22} \sim C_1 \frac{\bar{Y}^2}{\bar{X}^4}. \quad (17)$$

## Wall Boundary Layer: Self-Similar Solution

The boundary layer equations are invariant under a one parameter scaling group. This observation motivates the choice of similarity solution

$$\xi = \frac{\bar{Y}}{\bar{X}^2}, \quad \bar{\Psi} = \bar{X}^3 f(\xi), \quad \bar{p} = p_0 \bar{X}^{-2}, \quad \bar{T}_{11} = \bar{X}^{-2} t_{11}(\xi), \quad \bar{T}_{12} = \bar{X}^{-1} t_{12}(\xi), \quad \bar{T}_{22} = t_{22}(\xi), \quad (18)$$

which gives

$$0 = -2(t_{11} - p_0) - 2\xi t'_{11} + t'_{12}, \quad (19)$$

$$t_{11} + (-3f t'_{11} - 4f' t_{11} - 2f'' t_{12} + 4\xi f'' t_{11}) = 0, \quad (20)$$

$$t_{22} + (-3f t'_{22} + 4(3f - 3\xi f' + 2\xi^2 f'') t_{12} + 2(t_{22} + 1)(f' - 2\xi f'')) = 0, \quad (21)$$

$$t_{12} + (-3f t'_{12} - f' t_{12} + 2(3f - 3\xi f' + 2\xi^2 f'') t_{11} - (t_{22} + 1)f'') = 0, \quad (22)$$

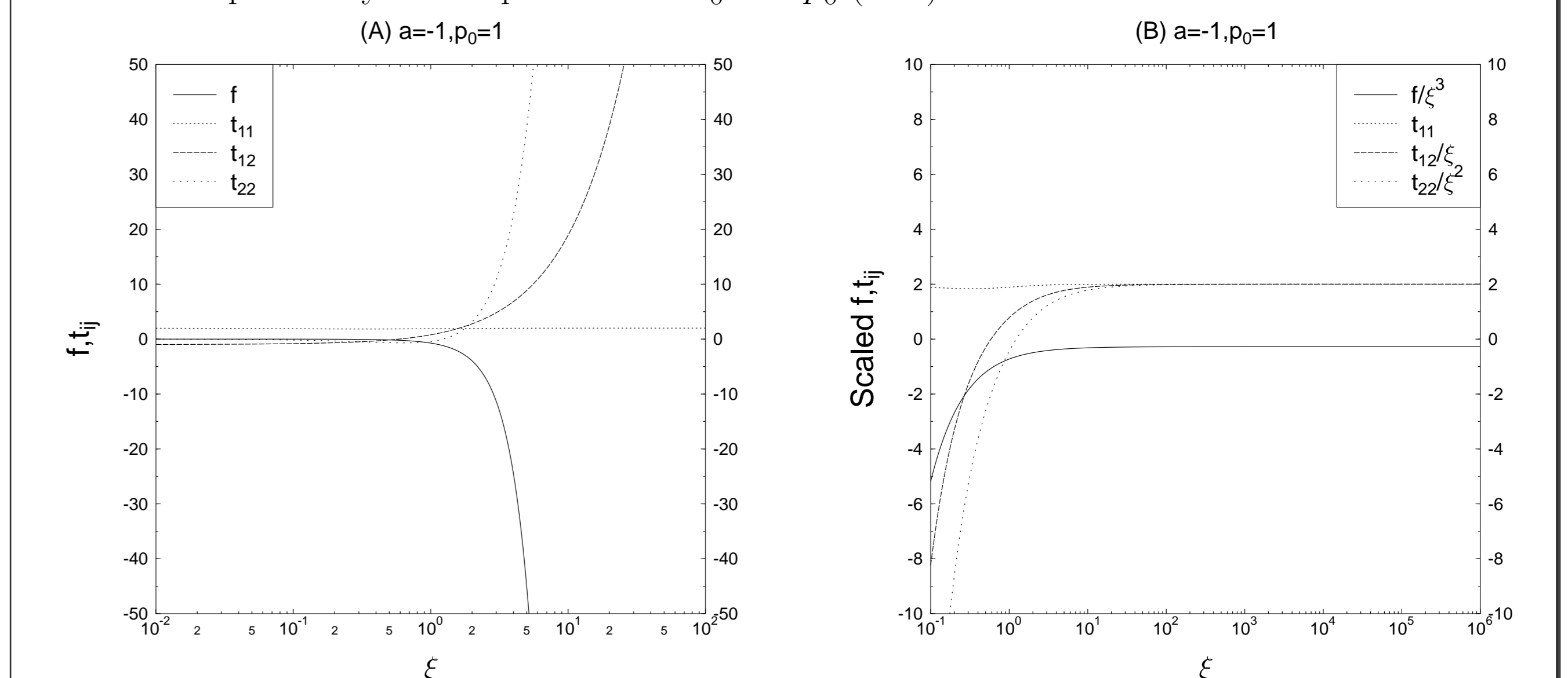
$$\text{at } \xi = 0: \quad f = f' = 0, \quad (23)$$

$$\text{as } \xi \rightarrow \infty: \quad f \sim C_0 \xi^3, \quad t_{11} \sim C_1, \quad t_{12} \sim C_1 \xi, \quad t_{22} \sim C_1 \xi^2. \quad (24)$$

The far-field behavior relates  $C_1$  and  $p_0$  through  $C_1 = 2p_0$ . Local analysis at  $\xi = 0$  for viscometric behavior at the wall shows that

$$f(\xi) \sim \frac{1}{2} a \xi^2, \quad t_{11}(\xi) \sim 2a^2, \quad t_{12}(\xi) \sim a, \quad t_{22}(\xi) \sim 2a\xi \quad \text{as } \xi \rightarrow 0, \quad (25)$$

where  $a = f''(0)$  is a free constant. An additional scaling invariance may be exploited to reduce the parameter dependence to the similarity variable  $a/p_0^{1/2}$ . Effectively, the wall boundary layer solutions depend only on the parameters  $C_0$  and  $p_0$  (or  $a$ ).



The wall boundary layer equations can now be solved as an initial value problem for an ordinary differential equation (see Fig. A). Convergence to the correct far-field behavior is demonstrated in Fig. B.

## UCM Solution Summary

The leading order core flow outer solution may be summarized as

$$v_r = \frac{g'(\theta)}{r}, \quad v_\theta = 0, \quad p = \frac{p_0}{r^2}, \quad T_{rr} = \frac{1}{r^2} (2p_0 + \text{Re } g'(\theta)^2), \quad T_{r\theta} = T_{\theta\theta} = 0, \quad (26)$$

valid for  $r = o(1)$  distances away from the walls. The function  $g(\theta)$  is arbitrary and set by the flow in  $r = O(1)$ . The only restriction is its wall behavior (10), dictated by the single layer boundary structure. Both undetermined parameters ( $C_0$  and  $p_0$  or  $a$ ) are set by the flow at  $r = O(1)$ . Similar results hold true for the case of Oldroyd-B fluids, see [1], and are likely to remain correct for other viscoelastic fluids with known boundary layer structure (such as Phan-Thien-Tanner fluids, see [3]). **No attempt has been made to study solutions with recirculating streamlines.**

## References

- [1] J.D. Evans and T. Hagen, *J. Non-Newtonian Fluid Mech.* **154** (2008), 39–46.
- [2] H. Giesekus, *Rheol. Acta* **7** (1968), 127–138.
- [3] T. Hagen and M. Renardy, *J. Non-Newtonian Fluid Mech.* **73** (1997), 181–189.
- [4] E. J. Hinch, *J. Non-Newtonian Fluid Mech.* **50** (1993), 161–171.
- [5] A. M. Hull, *J. Non-Newtonian Fluid Mech.* **8** (1981), 327–336.
- [6] M. Renardy, *J. Non-Newtonian Fluid Mech.* **58** (1995), 83–89.
- [7] M. Renardy, *J. Non-Newtonian Fluid Mech.* **68** (1997), 125–132.